Iranian Journal of Oil & Gas Science and Technology, Vol. 8 (2019), No. 3, pp. 101-112
http://ijogst.put.ac.ir

Thermodynamic and Kinetic Investigations of Corrosion Inhibition Behavior of 2-MBT on Steel at a pH of 8

Hojatallah Koraee[1], Hadi Eskandari[2], and Iman Danaee[3*]

[1] M.S. Student, Department of Chemical Engineering, Mahshahr Branch, Islamic Azad University, Mahshahr, Iran
[2] Assistant Professor, Department of Technical Inspection, Petroleum University of Technology, Abadan, Iran
[3] Associate Professor, Department of Technical Inspection, Petroleum University of Technology, Abadan, Iran

Received: April 16, 2015; *revised*: April 21, 2015; *accepted*: July 04, 2015

Abstract

Corrosion results in hazardous and expensive damage to pipelines, vehicles, water and wastewater systems, and even home appliances. One of the most extensively practical methods for protecting metals and alloys against corrosion is to use organic inhibitors. The inhibition capability of 2-Mercaptobenzothiazole (2-MBT) against the corrosion of carbon steel in a 2 M NaCl solution was examined by Tafel polarization. By using 2-Mercaptobenzothiazole both the cathodic and anodic reactions are delayed through chemical and physical adsorption and blocking the active corrosion sites. Based on the polarization curves, it was indicated that by increasing the inhibitor concentration, the inhibition efficiency increases up to 70% at room temperature, and it improves at higher temperatures. The adsorption of 2-Mercaptobenzothiazole was based on the Langmuir adsorption isotherm. The enthalpies of activation were determined to be around +50 $kJ.mol^{-1}$. The endothermic nature of the steel dissolution procedure is reflected by the positive symbols of the enthalpies (ΔH) of activation process. The determined ΔG_{ads} values range from -32.69 to -35.81 $kJ.mol^{-1}$, which shows both electrostatic adsorption and the chemisorption of the adsorption mechanism. The calculated entropy of adsorption was 78 $J.mol^{-1}.K^{-1}$ indicating the increment in the solvent entropy and a more positive water desorption entropy.

Keywords: Polarization, Corrosion Inhibitor, Adsorption, Steel

1. Introduction

Corrosion is a logically happening phenomenon which, due to a reaction with its environment, depreciates a metallic material or its features. Serious and expensive damage are caused by corrosion in different structures such as pipelines, public buildings and bridges, vehicles, water and wastewater systems, and even home appliances. It is one of the most severe problems in the oil and gas industry too. For protecting metals and alloys against corrosion, the use of organic inhibitors is a key practical method, since, by adding inhibitors, the industrial process is not disrupted (El-Taib Heakal et al., 2011). It has been demonstrated that sulfur- and/or nitrogen-containing heterocyclic compounds with different substituents are considered as the operative corrosion inhibitors in various solutions over a wide pH range (El-Taib Heakal et al., 2011). To reduce the oxidation or/and reduction corrosion reactions, an inhibitor must travel in water molecules from the metal surface and interact with anodic or/and cathodic reaction sites to prevent the transportation of water and corrosion active species on the surface.

---

[*] Corresponding author:
Email: danaee@put.ac.ir

Normally, the ability of an organic compound to inhibit corrosion is influenced by its efficiency to adsorb on a metal surface. The nature of the metal surface and the electronic structure of inhibiting molecules affect the protective nature of the adsorbed compact barrier film (El-Taib Heakal et al., 2011). The functional groups attached to aromatic rings contribute to the adsorption of the organic compounds (Shukla et al., 2010). Through blocking the active surface sites, these compounds reduce the corrosion rate. Organic inhibitors can cause four kinds of adsorption at a metal/solution interface: 1. electrostatic attraction between the charged molecules and charged metal, 2. interaction between metal and uncharged electron pairs in the molecule, 3. interaction between metal and p-electrons, and 4 a combination of the first and third adsorption methods (Naqvi et al., 2011). In the present work, the inhibitive effect 2-Mercaptobenzothiazole is investigated for C-steel corrosion in NaCl solutions using Tafel polarization method. The impacts of inhibitor concentration and temperature on the effectiveness of the examined compound and on the corrosion inhibition behavior were studied. Using the following equations, the degree of surface coverage (θ) and inhibition efficiency are determined at different concentrations of inhibitor (Hosseini et al., 2008; Negm et al., 2010)

$$\theta = \left[\frac{I^o_{corr} - I_{corr}}{I^o_{corr}}\right] \tag{1}$$

$$IE = \left[\frac{I^o_{corr} - I_{corr}}{I^o_{corr}}\right] \times 100 \tag{2}$$

where, IE represents the inhibition efficiency; I^o_{corr} and I_{corr} stand for the corrosion current densities calculated by the intersection of the extrapolated Tafel lines and the corrosion potential for mild steel in uninhibited and inhibited NaCl solutions respectively.

Polarization resistance (R_p) values were obtained from the slope of the polarization curve and calculated utilizing Stern–Geary equation as follows (Migahed et al., 2008; Keles et al., 2011):

$$R_p = \frac{\beta_a . \beta_c}{2.303(\beta_a + \beta_c) . I_{corr}} \tag{3}$$

By raising temperature from the normal point, the thermodynamic elements of activation procedure and adsorption can be determined at various concentrations of inhibitor. Based on Arrhenius equation, the apparent activation energy (E_a) of metal corrosion in both media (blank/uninhibited and inhibited) can be determined as follows (Herrag et al., 2010):

$$I_{corr} = A \, exp\left(\frac{-E_a}{RT}\right) \tag{4}$$

$$I_{corr} = \frac{RT}{Nh} exp\left(\frac{\Delta S}{R}\right) exp\left(\frac{-\Delta H}{RT}\right) \tag{5}$$

where, E_a is the apparent activation energy of corrosion and *R* is the universal gas constant; *A* represents the Arrhenius pre-exponential factor, and *h* stands for the Plank's constant; *N* shows the Avogadro Number; ΔS and ΔH represent the entropy of activation and the enthalpy of activation.

2. Experimental methods

2.1. Materials

In all the tests, a three-electrode glass cell was utilized. As the counter electrode and reference electrode, a platinum electrode and a saturated calomel electrode (SCE) were used respectively. The working electrode (WE) was considered in the shape of a disc cut of steel with a geometric area of 1 cm^2. To ensure the same surface roughness, the test electrode was first polished using 1000 and 1500 grade emery paper, and was then rinsed with distilled water. The open circuit potential (OCP) of the working electrode was determined vs. time until achieving a quasi-stationary value before the polarization experiments.

The tests were performed in a stagnant 2 M NaCl solution without any inhibitor and in the presence of various concentrations of 2-Mercaptobensothiazole as a corrosion inhibitor. Figure 1 represents the molecular structure of 2-MBT. All the prepared chemicals having a reagent grade (Merck) were utilized without more purification, and all the solutions were prepared using distilled water. The tests were conducted at various temperatures of 25, 45, and 65 °C.

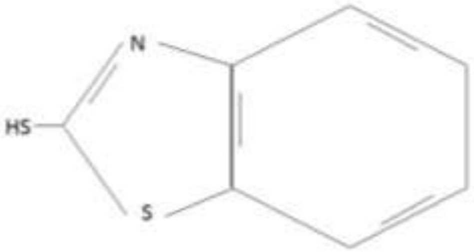

Figure 1

The chemical structure or 2-Mercaptobenzothiazole.

2.2. Methods

Using an electrochemical measurement system, polarization curves were recorded (potentiostat–galvanostat model Autolab controlled by a PC equipped with the Nova1.8 Software). Polarization curves vs. SCE were recorded at a constant sweep rate of 1 $mV.s^{-1}$ from -250 mV to +250 mV. From the Tafel region of cathodic and anodic branch of polarization curves, the cathodic and anodic Tafel slops (β_c and β_a) were determined respectively.

3. Result and discussion

3.1. Potentiodynamic polarization measurements

Anodic and cathodic polarization plots of mild steel are presented in Figure 2 in a 2 M NaCl solution with and without 2-Mercaptobenzothiazole at different concentrations and at various temperatures of 25, 45, and 65 °C. The electrochemical corrosion kinetic parameters, including corrosion potential (E_{corr} vs. SCE), cathodic and anodic Tafel slopes (β_a and β_c), corrosion current density (I_{corr}), surface coverage degree (Θ), and inhibition efficiency (*IE*) provided by the extrapolation of the Tafel lines are tabulated in Table 1.

Both cathodic and anodic currents decrease by adding 2-Mercaptobenzothiazole to the corrosive media. The existence of the inhibitor results in the reduction in the corrosion current density and corrosion rate of steel. However, the corrosion potential nearly remains the same compared to the blank solution.

These findings represent that 2-MBT can be categorized as a mixed-type corrosion inhibitor. In the presence of inhibitor, the cathodic branches show the parallel lines indicating that the hydrogen evolution mechanism is not modified by raising 2-Mercaptobenzothiazole concentration, and the reduction at steel surface is controlled by charge transfer (Hoseinzadeh et al., 2013).

According to Table 1, the reduction in either I_{corr} or the corrosion rate (CR) at an incremented concentration is mostly caused by an increase in the polarization resistance (R_p).

Table 1

Electrochemical parameters obtained from the polarization curves of the 2-Mercaptobenzothiazole at different temperatures.

Temperature (C)	Concentration (M)	(µA.cm^{-2})	(mV vs. SCE)	(mV.dec^{-1}	β_A (mV.dec^{-1}	(Ω cm^2)	(%)	θ	Corrosion Rate (Mpy)
25	0	2.51	420	162	153	13.61	_	_	1.147
	1×10^{-4}	1.348	440	140	130	21.71	46.29	0.4629	0.616
	3×10^{-4}	1.122	430	122	117	23.11	55.29	0.5529	0.512
	5×10^{-4}	0.912	430	118	123	28.67	63.66	0.6366	0.416
	1×10^{-3}	0.95	450	121	118	27.30	62.15	0.6215	0.434
	2×10^{-3}	0.79	450	92	90	25	68.52	0.6852	0.361
45	0	11.22	420	122	119	2.331	_	_	5.127
	1×10^{-4}	6.30	460	118	108	3.886	43.85	0.4385	2.87
	3×10^{-4}	3.98	380	114	105	5.96	64.52	0.6452	1.818
	5×10^{-4}	3.71	410	86	85	5.003	66.93	0.6693	1.695
	1×10^{-3}	2.08	430	110	96	10.702	81.46	0.8146	0.95
	2×10^{-3}	1.86	420	99	77	10.11	83.42	0.8342	0.85
65	0	39.81	390	130	103	0.626	_	_	18.19
	1×10^{-4}	26.30	400	111	102	0.877	33.93	0.3393	12.01
	3×10^{-4}	13.80	390	102	99	1.20	65.33	0.6533	6.30
	5×10^{-4}	10	420	81	74	1.67	74.88	0.7488	4.57
	1×10^{-3}	10.47	420	75	83	1.63	73.70	0.7370	4.78
	2×10^{-3}	5.88	390	73	70	2.638	85.22	0.8522	2.68

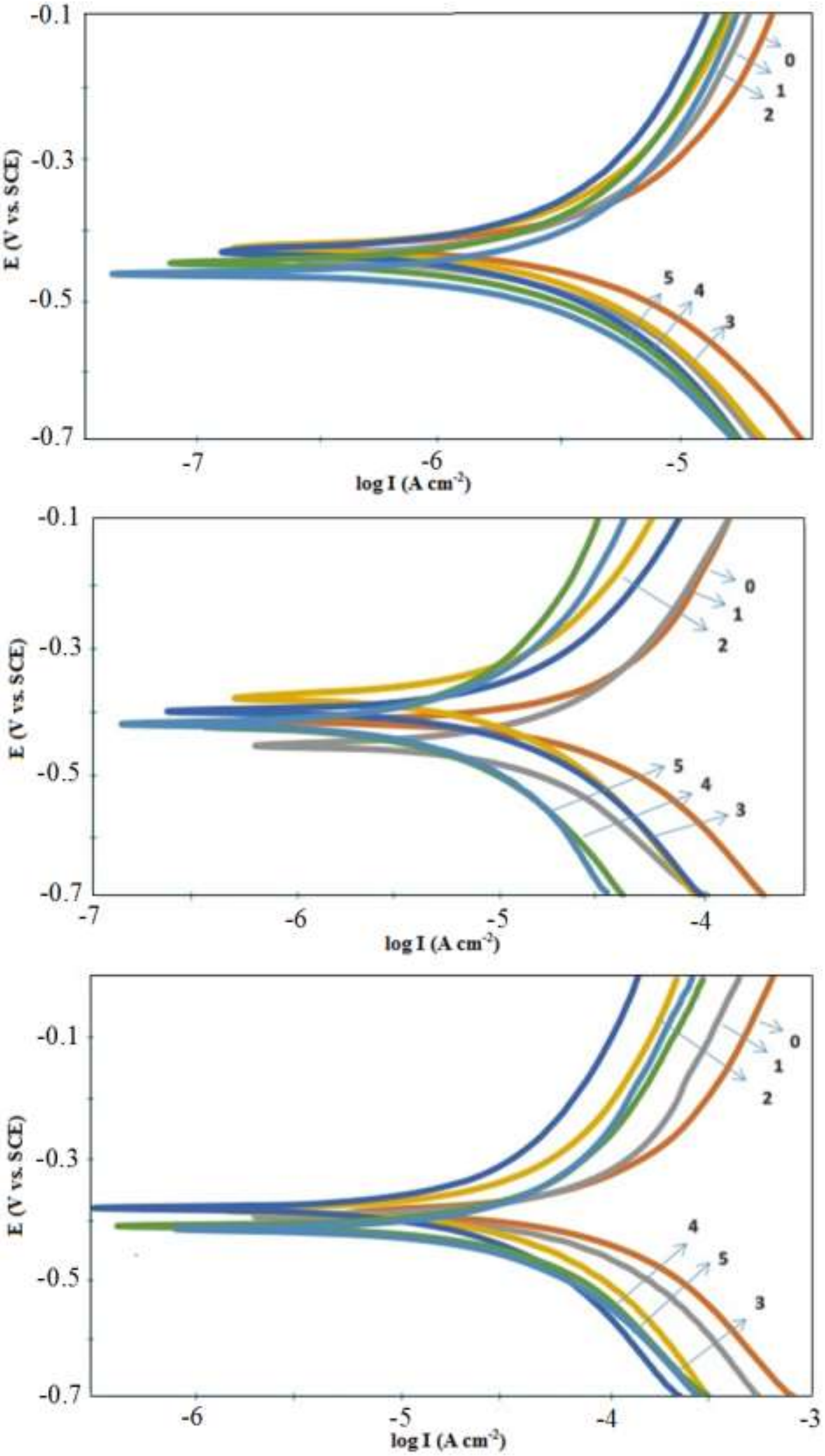

Figure 2

Anodic and cathodic polarization curves (Tafel curves) for steel in a 2 M NaCl solution at different temperatures of a) 25 °C, b) 45 °C, and 65 °C; and at various concentration of 2-Mercaptobbenzothiazole: 1) 0, 2) 1×10^{-4}, 3) 3×10^{-4}, 4) 5×10^{-4}, 5) 1×10^{-3}, and 6) 1×10^{-3} M.

3.2. Effect of temperature

The change in corrosion rate versus temperature was also investigated with and without 2-MBT in a 2 M NaCl solution. Hence, polarization readings were conducted at various temperatures at different concentrations of 2-Mercaptobenzothiazole (Figure 2). In addition, Tables 1 lists the extracted and summarized electrochemical elements. It is evident that by incrementing temperature in both solutions, both I_{corr} values and efficiency values increase. According to Figure 2, increasing temperature does not significantly affect the corrosion potentials; however, it leads to a higher corrosion rate (I_{corr}).

Figure 3 depicts the Arrhenius plots for the corrosion rate of steel. From the slope of ln (I_{corr}) versus 1/T plots, the values of apparent activation energy of corrosion (E_a) were calculated for mild steel in a 2 M NaCl solution at different concentrations of 2-Mercaptobenzothiazole as also represented in Table 2. Radovici reported that a decrease in E_a in the presence of the inhibitor compared to blank solution led to chemisorption (Hoseinzadeh, et al.2013). The chemical adsorption is caused by creating a coordinated bond between the *d*-orbital of iron and inhibitor molecules on the surface of steel via a lone pair of electrons of N, S, and/or O atoms. It was explained by Szauer and Brand that the reduction in activation energy can be attributed to a significant increment in the adsorption of inhibitor on the steel surface at an increased temperature.

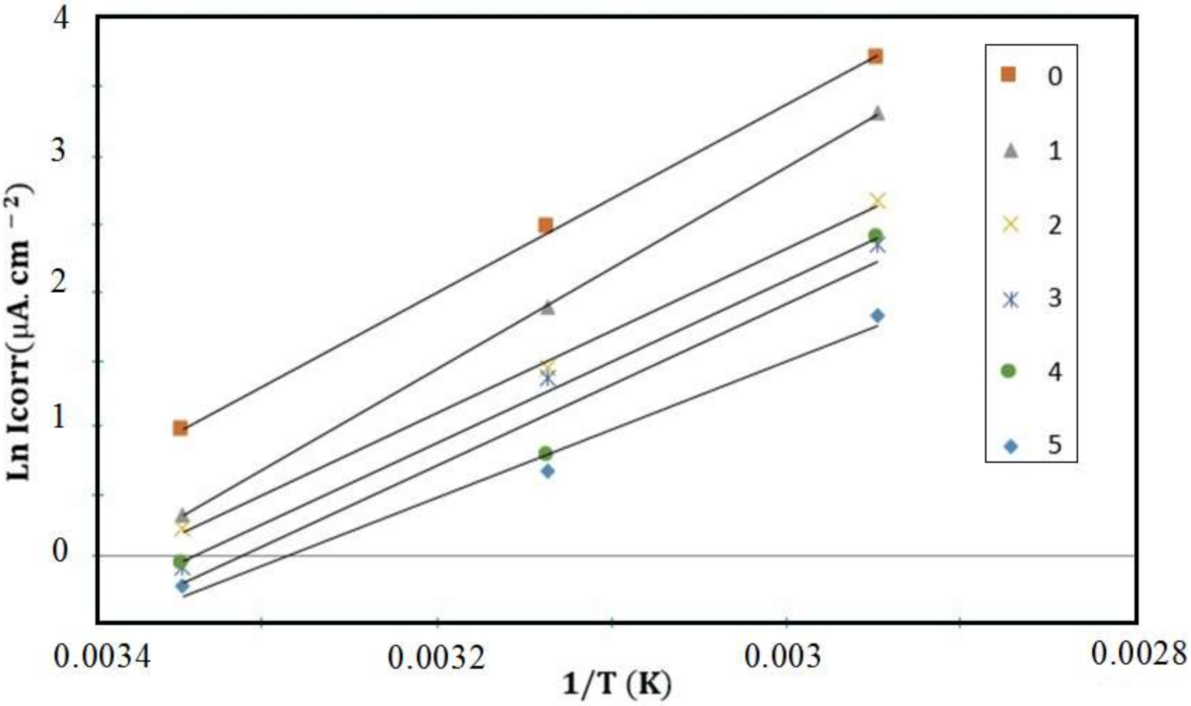

Figure 3

Arrhenius plots of steel corrosion rates (I_{corr}) in a 2 M NaCl solution at different concentrations of 2-Mercaptobenzothiazole: 0) 0, 1) 1×10^{-4}, 2) 3×10^{-4}, 3) 5×10^{-4}, 4) 1×10^{-3}, and 5) 1×10^{-3} M.

A plot of ln(I_{corr}/T) against 1/T is provided in Figure 4. Table 2 also represents the values of ΔH and ΔS obtained from the straight lines with a slope of ($-\Delta H/R$) and an intercept of ln(R/Nh) + $\Delta S/R$. In the system, the endothermic nature of the steel dissolution process is reflected by the positive symbols of the enthalpies (ΔH). It is inferred from the negative values of entropies that the activated complex in the rate determining phase shows a relation rather than a dissociation step, meaning a reduction in disordering on going from reactants to the activated complex (Herrag et al., 2010). Table 2 lists the values of the standard free energy of activation, $\Delta G = \Delta H - T\Delta S$, at various temperatures. The positive values of ΔH and ΔG indicate an endothermic process of the dissolution reaction in the NaCl solution.

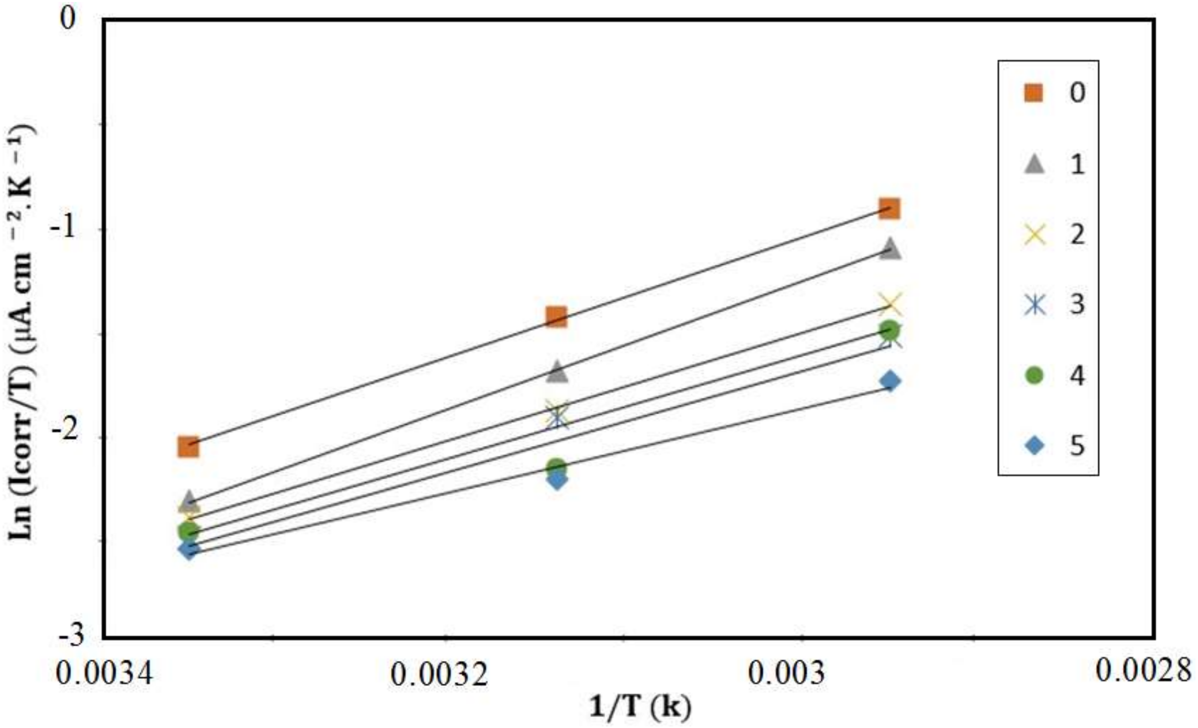

Figure 4

Typical Arrhenius plots of $\ln(I_{corr}/T)$ vs $1/T$ for carbon steel in a 2 M NaCl solution at different concentrations of 2-Mercaptobenzothiazole: 0) 0, 1) 1×10^{-4}, 2) 3×10^{-4}, 3) 5×10^{-4}, 4) 1×10^{-3}, and 5) 1×10^{-3} M.

Table 2

Corrosion kinetic parameters for steel in a 2 M NaCl solution at different concentrations of 2-Mercaptobenzothiazole.

Concentration (M)	E_a (kJ.mol^{-1})	A (μA.cm^{-2})	ΔH (kJ.mol^{-1})	ΔS (kJ.mol^{-1}.K^{-1})	ΔG (kJ.mol^{-1})		
					25 °C	45 °C	65 °C
0	57.42	7.20×10^{10}	55.02	-0.055	71.41	72.51	73.61
1×10^{-4}	61.72	4.36×10^{10}	59.04	-0.051	72.24	75.26	76.28
3×10^{-4}	50.40	4.85×10^{8}	49.75	-0.074	71.81	73.29	74.77
5×10^{-4}	49.69	1.08×10^{8}	47.36	-0.090	74.19	75.99	77.79
1×10^{-3}	49.83	2.94×10^{8}	46.88	-0.086	72.52	74.24	75.96
2×10^{-3}	41.67	6.56×10^{7}	38.75	-0.113	72.44	74.70	76.96

3.3. Thermodynamic adsorption parameters

Through adsorption isotherm, basic thermodynamic information on the interaction between metal surface and inhibitor molecules can be provided which is utilized for the thermodynamic calculations of inhibitor adsorption (Betiss et al., 2005). Various adsorption isotherms, including Langmuir, Temkin, Ei-Away, Bockris-Swinkels, Flory-Huggins, and Frumkin exist (Ghanbari et al., 2010). By exploiting the thermodynamic data obtained from the isotherms, the kind of inhibitor adsorption, i.e. chemisorption or physisorption, can be distinguished. The exchange of water molecules with inhibitor molecules on the metal surface can show the organic inhibitor adsorption at the metal/solution interface (Aljourani et al., 2009).

$Org_{(sol)} + nH_2O_{(ads)} \rightarrow Org_{(ads)} + nH_2O_{(sol)}$

where, $Org_{(sol)}$ is inhibitor molecules dissolved in solution, and $Org_{(ads)}$ represents inhibitor molecules adsorbed on the metal surface. Moreover, $H_2O_{(sol)}$ and $H_2O_{(ads)}$ respectively are the water molecules and water molecules adsorbed on the metal surface in solution, and *n* stands for the size ratio indicating the number of water molecules exchanged for inhibitor molecules.

Numerous adsorption isotherms, including Freundlich, Temkin, Flory–Huggins, and Langmuir isotherms were evaluated to explain the adsorption of 2-Mercaptobenzothiazole on the steel surface. Employing the Langmuir adsorption isothermal equation, the best agreement was obtained as follows:

$$\frac{C_{inh}}{\theta} = \frac{1}{K_{ads}} + C_{inh} \tag{6}$$

where, C_{inh} represents the concentration of the inhibitor, and K_{ads} is the adsorptive equilibrium constant; θ also shows the degree of the surface coverage of inhibitor molecules. According to Figure 4, the plot of $\frac{C_{inh}}{\theta}$ versus C_{inh} leads to a straight line with a correlation coefficient of over 0.99, indicating that the adsorption of these inhibitors matches Langmuir adsorption isotherm in an acidic solution.

K_{ads} values can be obtained from the intercept of $\frac{C_{inh}}{\theta}$ versus C_{inh} curves (see Figure 5). K_{ads} is associated with the standard free energy of adsorption using the following equation (Herrag et al., 2010).

$$\Delta G_{ads} = -RT\, ln(55.5\, K_{ads}) \tag{7}$$

where, the constant 55.5 represents the molar concentration of water in solution, and *R* is the universal gas constant. Using Equation 7, various values of ΔG_{ads} for 2-Mercaptobenzothiazole were obtained as a function of temperature in the range of 298–323 K. Table 3 summarizes the determined values of K_{ads} and ΔG_{ads} at various temperatures.

Table 3

Thermodynamic parameters of the adsorption of 2-Mercaptobenzothiazole on the steel in a 2 M NaCl solution at different temperatures.

T (K)	$\boldsymbol{K_{ads}}$ (M^{-1})	$\Delta \boldsymbol{G_{ads}}$ (kJ.mol^{-1})
298.15	9708	-32.69
318.15	7575	-34.23
338.15	6172	-35.81

The negative sign and high values of K_{ads} show that 2-Mercaptobenzothiazole molecules are intensely and immediately adsorbed on the steel surface. In general, the absolute values of ΔG_{ads} up to 20 kJ.mol^{-1} are in agreement with physisorption while those around 40 kJ.mol^{-1} or higher are related to chemisorption. This is caused by sharing or transferring of electrons from organic molecules to the metal surface to create a coordinate kind of metal bonds (Outirite et al., 2010). Herein, the calculated ΔG_{ads} values range from -32.69 to -35.81 kJ.mol^{-1}, which indicates that the adsorption mechanism of 2-Mercaptobenzothiazole is both electrostatic adsorption (ionic) and chemisorption (molecular) on mild steel in a 2 M NaCl solution at the considered temperatures (Ali et al., 2008). Coordinate covalent bonds can be formed between the electron pairs of unprotonated N atom and S atom of the thiazole ring and the metal surface (Hoseinzadeh et al., 2013).

Using the enthalpy (ΔH_{ads}) and entropy (ΔS_{ads}) of adsorption, the corrosion inhibition of 2-Mercaptobenzothiazole for steel can be better clarified; to this end, the following integrated van’t Hoff equation is used:

$$lnK_{ads} = -\frac{\Delta H_{ads}}{RT} + \frac{\Delta S_{ads}}{R} + ln\frac{1}{55.5} \quad (8)$$

By plotting $\ln K_{ads}$ against $1/T$, the enthalpy and entropy of adsorption can be obtained. The straight lines are achieved at an intercept equal to $\frac{\Delta S_{ads}}{R} + \ln\frac{1}{55.5}$ and at a slope equal to $-\frac{\Delta H_{ads}}{R}$. Table 4 tabulates the calculated values of the entropy of adsorption and the heat of adsorption. Furthermore, to calculate the enthalpy of adsorption, Gibbs-Helmholtz equation can be used (Noor et al., 2007):

$$\left(\frac{\partial\left(\frac{\Delta G}{T}\right)}{\partial T}\right)_p = -\frac{\Delta H}{T^2} \quad (9)$$

Integrating Equation 9 can lead to:

$$\frac{\Delta G_{ads}}{T} = \frac{\Delta H_{ads}}{T} + constant \quad (10)$$

The obtained value of ΔH_{ads} is listed in Table 4. It is observed that the value of the enthalpy of adsorption in Gibbs-Helmholtz equation is consistent with the one obtained via van’t Hoff equation. As observed in Table 4, the positive symbol of ΔS_{ads} indicates the substitution process, which can be recognized by the increased solvent entropy and more positive water desorption entropy. It is also explained by an increment in disorders caused by more water molecules, which can be desorbed from the metal surface via one inhibitor molecule (Donahue et al., 1965). An endothermic adsorption process ($\Delta H_{ads} > 0$) is ascribed unequivocally to chemisorption, and either physisorption, or chemisorption, or a mixture of both processes may be involved in an exothermic adsorption process ($\Delta H_{ads} < 0$). According to the results of this work, it is inferred from the calculated ΔG_{ads} and ΔH_{ads} values of 2-Mercaptobenzothiazole that the adsorption mechanism is not entirely physical or chemical, and there is a combination of physisorption and chemisorption at the inhibitor and metal surface (Jafari et al., 2013).

Table 4

Thermodynamic and equilibrium adsorption parameters of the adsorption of 2-Mercaptobenzothiazole on the steel surface in a 2 M NaCl solution.

Different thermodynamic equations	ΔH_{ads} (kJ.mol^{-1})	ΔS_{ads} (kJ.mol^{-1}.K^{-1})
Gibbs-Helmholtz equation	-9.25	-
van’t Hoff equation	-9.56	0.078

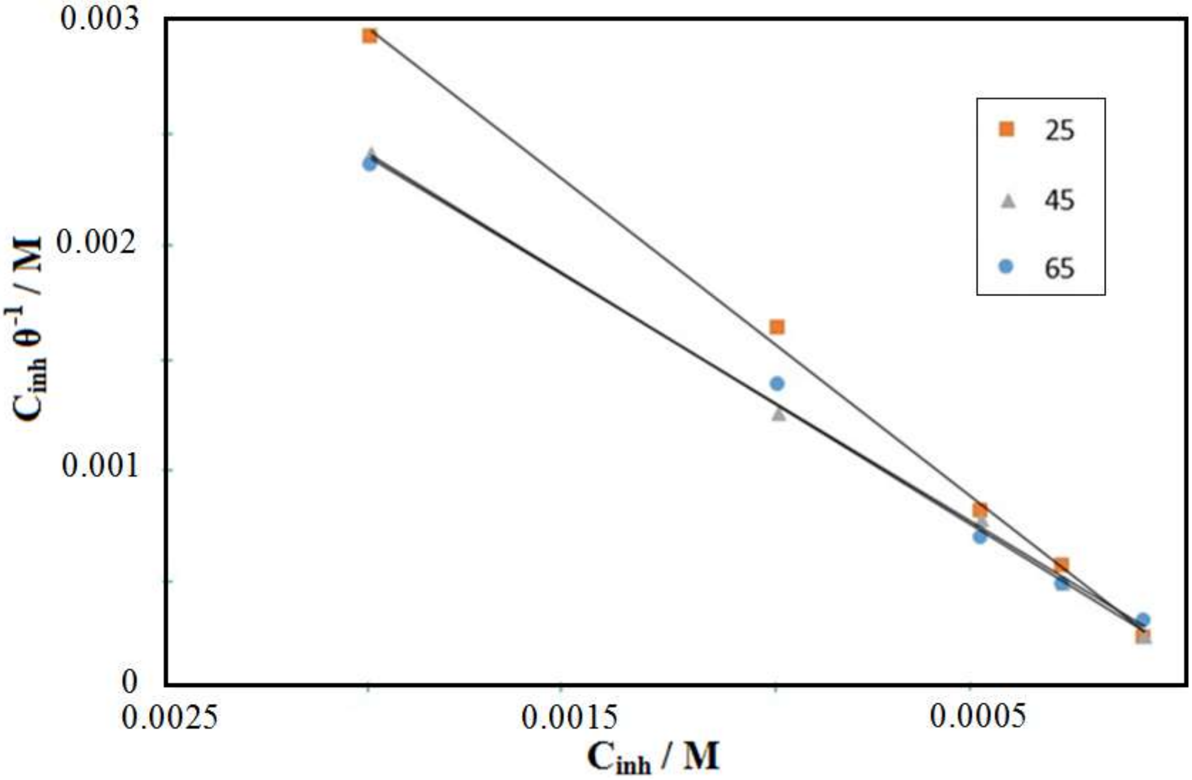

Figure 5

Langmuir isotherm adsorption model of 2-Mercaptobenzothiazole on the surface of steel in a 2 M NaCl solution.

4. Conclusions

1. 2-Mercaptobenzothiazole plays a key inhibition role in the corrosion of carbon steel in a 2 M NaCl solution. Its inhibition efficiency depends both on the concentration of the inhibitor and temperature. By increasing the inhibitor concentration up to 70% and increasing temperature, the inhibition efficiency rises.
2. By incrementing the temperature, corrosion current density is increased; however, the corrosion rate is lower when 2-Mercaptobenzothiazole is used.
3. It is demonstrated in the polarization measurements that 2-Mercaptobenzothiazole, by inhibiting both the anodic metal dissolution and the cathodic reactions, shows a behavior similar to a mixed-type corrosion inhibitor.
4. Through Langmuir adsorption isotherm, the adsorption of 2-Mercaptobenzothiazole molecules on carbon steel surface was explained. The values of K_{ads} and ΔG_{ads} were determined to be around 7×10^3 and -34 kJ.mol^{-1} respectively. By employing thermodynamic adsorption elements, it was shown that through a spontaneous exothermic procedure, the inhibitor is adsorbed, and both physisorption and chemisorption processes can be proposed for this compound.

The entropy of adsorption was calculated to be 78 J.mol^{-1}.K^{-1}. With the positive value of entropy, an increased solvent entropy and further positive water desorption entropy were indicated. The enthalpies of the activation procedure were computed to be about +50 kJ.mol^{-1}, representing the endothermic nature of the steel dissolution procedure.

References

Aljourani, J., Raeissi, K., and Golozar, M.A., Benzimidazole and its Derivatives as Corrosion Inhibitors for Mild Steel in 1 M HCl Solution, Corrosion Science, Vol. 51, No. 8, p. 1836-1843, 2009.

Ali, S.A., Al-Muallem, H.A., Saeed, M.T., and Rahman, S.U., Hydrophobic-tailed Bicycloisoxazolidines: A Comparative Study of the Newly Synthesized Compounds on the Inhibition of Mild Steel Corrosion in Hydrochloric and Sulfuric Acid Media, Corrosion Science, Vol. 50, No. 3, p. 664-675, 2008.

Betiss, F., Lebrini, M., and Lagrenee, M., Thermodynamic Characterization of Metal Dissolution and Inhibitor Adsorption Processes in Mild Steel/2,5-Bis(N-Thienyl)-1,3,4 Thiadiazoles/Hydrochloric Acid System, Corrosion Science, Vol. 47, No. 12, p. 2915-2931, 2005.

Donahue, F. M. and Nobe, K. , Theory of Organic Theory of Corrosion Inhibitors: Adsorption and Linear Free Energy Relationships, Journal of the Electrochemical Society, Vol. 112, No. 1, p. 886-891, 1965.

El-Taib Heakal, F., Fouda, A. S., and Radwan, M. S., Inhibitive Effect of some Thiadiazole Derivatives on C-Steel Corrosion in Neutral Sodium Chloride Solution, Material Chemistry and Physics, Vol. 125, No. 1-2, p. 26–36, 2011.

Ghanbari, A., Attar, M. M., and Mahdavian, M., Corrosion Inhibition Performance of Three Imidazole Derivatives on Mild Steel in 1 M Phosphoric Acid, Material Chemistry and Physics, Vol. 124, No. 2-3, p. 1205-1209, 2010.

Hosseini, S.M.A. and Azimi, A., The Inhibition Effect of the New Schiff Base, Namely 2,20-[Bis-N(4-Choloro Benzaldimin)]-1, 10-Dithio against Mild Steel Corrosion, Material and Corrosion, Vol. 59, No. 1, p. 41–45, 2008.

Hoseinzadeh, A.R., Danaee, I., and Maddahy, M.H., Thermodynamic and Adsorption Behavior of Vitamin B1 as a Corrosion Inhibitor for AISI 4130 Steel Alloy in HCl Solution, Zeitschrift Für Physikalische Chemie Vol. 227, No. 4, p. 403-417, 2013.

Herrag, L., Hammouti, B., Elkadiri, S., Aouniti, A., Jama, C., Vezin, H., and Bentiss, F., Adsorption Properties and Inhibition of Mild Steel Corrosion in Hydrochloric Solution by some Newly Synthesized Diamine Derivatives: Experimental and Theoretical Investigations, Corrosion Science, Vol. 52, No. 9, p. 3042–3051, 2010.

Jafari, H., Danaee, I., Eskandari, H., and Rashvandavei, M., Electrochemical and Theoretical Studies of Adsorption and Corrosion Inhibition of N,N′-Bis(2-Hydroxyethoxyacetophenone)-2,2-Dimethyl- 1,2-Propanediimine on Low Carbon Steel (API 5L Grade B) in Acidic Solution, Industrial and Engineering Chemistry Research, Vol. 52, No. 20, p. 6617-6632, 2013.

Keles, H., Electrochemical and Thermodynamic Studies to Evaluate Inhibition Effect of 2-[(4-Phenoxy-Phenylimino) Methyl]-Phenol in 1 M HCl on Mild Steel, Material Chemistry and Physics, Vol. 130, No. 3, p. 1317– 1324, 2011.

Migahed, M. A. and Nassar, I. F., Corrosion Inhibition of Tubing Steel During Acidization of Oil and Gas Wells, Electrochimica Acta, Vol. 53, No. 6, p. 2877-2882, 2008.

Naqvi, I., Saleemi, A.R., and Naveed, S., Cefixime: A Drug as Efficient Corrosion Inhibitor for Mild Steel in Acidic Media, International Journal of Electrochemical Science. Vol. 6, No. 3, p. 146-161, 2011.

Negm, N. A., Elkholy,Y. M., Zahran, M. K., and Tawfik, S. M., Corrosion Inhibition Efficiency and Surface Activity of Benzothiazol-3-Ium Cationic Schiff Base Derivatives in Hydrochloric Acid, Corrosion Science, Vol. 52, No. 10, p. 3523-3536, 2010.

Noor, E. A., Temperature Effects on the Corrosion Inhibition of Mild Steel in Acidic Solutions by Aqueous Extract of Fenugreek Leaves, International Journal of Electrochemical Science, Vol. 2, No. 4, p. 996-1017, 2007.

Outirite, M., Lagrenée, M., Lebrini, M., Traisnel, M. , Jama, C. , Vezin, H., and Bentiss, F., AC Impedance, X-Ray Photoelectron Spectroscopy and Density Functional Theory Studies of 3,5-Bis(N -Pyridyl)-1,2,4-Oxadiazoles as Efficient Corrosion Inhibitors for Carbon Steel Surface in Hydrochloric Acid Solution, Electrochimica Acta, Vol. 55, No. 5, p. 1670-1681, 2010.

Shukla, S.K. and Quraishi, M.A., The Effects of Pharmaceutically Active Compound Doxycycline on the Corrosion of Mild Steel in Hydrochloric Acid Solution, Corrosion Science, Vol. 52, No. 2, p. 314–321, 2010.